Finite temperature and confinement along the extra dimensions studied on a five-dimensional U(1) lattice gauge model

K. Farakos[*] and S. Vrentzos[†]

October 30, 2018

Physics Department, National Technical University of Athens,
Zografou Campus 15780, Greece

Abstract

In this paper we study the properties of the phase diagram of a simple extra dimensional model on the lattice at finite temperature. We consider the five-dimensional pure gauge abelian model with anisotropic couplings which at zero temperature exhibits a new interesting phase, the layer phase. This phase is characterized by a massless photon living on the four dimensional subspace and confinement along the extra dimension. We show that, as long as the temperature takes a non zero value the aforementioned layer phase disappears. It would be equivalent to assume that at finite temperature the higher-dimensional lattice model loses any feature of the layered structure due to the deconfinement which opens up the interactions between the three-dimensional subspaces at finite temperature.

[*]E-mail: kfarakos@central.ntua.gr
[†]E-mail: vrentsps@central.ntua.gr

1 Introduction

The original idea of Fu and Nielsen in the mid-eighties of the last century consisted in proposing a new way of dimensional reduction through higher dimensional lattice models with anisotropic couplings [1]. Since then in a series of papers the phase diagram of the higher-dimensional lattice models was studied by mean field and Monte carlo methods. Besides that a mechanism of producing the anisotropic couplings was proposed invoking a Randall-Sundrum space-time metric to the (continuum) higher dimensional models[2, 3]. The lattice model with anisotropic couplings which came up could help in understanding the localisation of the gauge interaction on the brane; the idea was that the usual four-dimensional space-time is embedded in a higher dimensional bulk in which the extra dimensions are subject to confinement. Indeed the assumed strong coupling dynamics along the extra dimension requires a non-perturbative study. The numerical study on the lattice has verified the prediction of a new phase (layer phase) proposed by Fu and Nielsen who used mean field methods. In this new phase we established the existence of a massless photon on the four-dimensional subspace while at the same time the extra dimension is confined [4]. This confinement is responsible for the fact that the higher-dimensional space is layered-like and the interactions are confined in the four-dimensional space-time slices.

It is worthwhile to mention that in the Dvali-Shifman model a similar way of thinking has been used in order to achieve a localization mechanism on a brane: the assumption of confinement (of a non-abelian nature) along one of the dimensions which limits the dynamics of the model in a subspace with one dimension less [5]. It is possible to generate gravitationally this localization mechanism for the trapping of the charged fields, under a non-abelian gauge field, on a 3d submanifold (brane) using the non-minimal coupling of gravity with a scalar field [6]. The result is a spontaneously broken phase on the brane (higgs phase) and a confining (symmetric phase) in the transverse directions (bulk).

In this work we consider the following exercise: we assume a five-dimensional U(1) lattice model with anisotropic couplings at finite temperature. Our intention is to discover the fate of the layer phase as we switch on the temperature to non zero values. By means of numerical methods we study the phase diagram and our main result is that for $T \neq 0$ the layer phase becomes a deconfined phase with new properties. In other words, the confining extra dimension that is detected at $T = 0$, becomes deconfined for non zero values of the temperature and the system is lacking the four-dimensional layered structure. [1]

The previous result is suggestive for the behavior of a multidimensional anisotropic gauge-higgs model at finite temperature [2]. It is well known that at high temperature the higgs phase turns into a symmetric phase. We expect then that the layer higgs phase disappears at this

---

[1]Our results contradict the prediction based on a Variational Cumulant Expansion by the authors of ref. [7] for which the layer phase of the anisotropic lattice gauge models persists at high temperature.

[2]For the analysis of anisotropic gauge-higgs models at zero temperature see the refs. [8, 9].

temperature. The new phase is probably a multidimensional high temperature symmetric phase: a hot multidimensional world in the "quark-gluon plasma" phase. In this rather hypothetical scenario the Universe starts as a hot multidimensional system that cools down, passes through a series of phase transitions and ends up to a brane Universe at zero temperature.

To explore the phase diagram of the anisotropic 5D U(1) gauge model we have to understand first the phase structure of the 4D U(1) gauge model at high temperature. The study of the phase structure of lattice electrodynamics in three and four dimensions at zero temperature, using the topological excitations of the theory (monopoles) was first performed by the authors of ref. [10]. Computer simulations for the 3D compact QED at finite temperature were performed in ref. [11] for the deconfinement transition from the monopole anti-monopole point of view. In three dimensions and zero temperature the theory is confining for all values of the coupling constant and a monopole and anti-monopole plasma is responsible for the permanent confinement of oppositely charged particles. For non-zero temperature the binding of monopoles and the formation of magnetic dipoles lead to loss of confinement. The dipole plasma can not sufficiently screen the field created by electric currents and the screening mass vanishes.

In four dimensions the point-like topological excitations become one-dimensional objects (strings of monopole currents). Again, in the zero-temperature case and for small values of the coupling constant β there is a large number of monopole loops winding around the system and causing disorder. As a consequence, if an external field is applied it will be shielded after a small penetration. For large values of β, on the other hand, the situation is different. A long distance penetration of the external field is observed, accompanied by the renormalization of the magnetic charges due to the monopole currents. The case of 4D compact U(1) gauge theory at finite temperature was studied separately in [12] and [13]. The authors of reference [12] reported a second order phase transition to a Coulomb phase for $L_t \geq 4$, with critical exponents consistent with 3d Gaussian values and no obvious dependence on L_t. A different picture emerged in ref. [13], where among other things the disappearance of the Coulomb phase for all values of $T(\equiv \frac{1}{L_t}) \neq 0$ was predicted. Instead of a Coulomb phase we are left with a spatial confining - temporal Coulomb phase for all temperatures.

In this paper, we are not going to present a detailed study of the nature of the phase transitions; however, some of our findings seem to indicate the absence of a Coulomb phase for all temperatures different from zero for the case of four dimensional compact QED (as long as the condition $L_t << L_s$ is satisfied). We go one step further and examine a finite temperature scenario in five dimensions through the anisotropic U(1) gauge model with couplings β and β'. The connection of this model with the brane model scenarios makes it an ideal candidate for the study of the brane models in the non-zero temperature case. We are mostly interested to discover if some of the most promising characteristics of this model survive in the high-temperature regime. In what follows we will try to give a brief summary of our findings

through the description of the limiting cases of our model.

For $\beta' = 0$ we obtain the four dimensional QED at finite temperature. From the study of the system with volume $V_{4D} = L_t \times L_s^3$ and $L_t = 2, 4$ and 6 we come to the conclusion that, although phase transitions seem to appear for finite L_s, they are actually finite-size effects and disappear in the limit $L_s \to \infty$. For all values of $L_t \neq 0$ the Coulomb phase gives its place to a temporal Coulomb - spatial confining phase (deconfining phase) [14]. The Coulomb phase is recovered only at $T = 0$.

For $\beta' \neq 0$ and $L_t = 2$ we have a five dimensional, anisotropic model in a high temperature state. The zero temperature model has been already studied and it is characterized by three distinct phases [3, 4, 15, 16]. A five dimensional confining phase, a 5D Coulomb phase and the layer phase where the system is confining along the fifth direction while, along the four remaining directions, it exhibits the Coulomb behaviour with a massless photon. These characteristics change when the temperature becomes non-zero. We observed the replacement of the layer phase by a deconfining phase, due to the same mechanism responsible for the disappearance of the Coulomb phase in four dimensions. The behavior of the system in the time direction is coulombic and confining in the remaining four directions.

Our work is organized as follows. In section 2 we present the action of the model and the observables, the helicity modulus and the Polyakov line, that we use in order to characterize the phase diagram of the model. In section 3 we analyze the system in the three limiting cases: 5D anisotropic for $T = 0$, $\beta' = 0$ and $L_t = 1$. Finally in section 4 we present the phase diagram for the 5D anisotropic model at finite temperature and in particular for $L_t = 2$. [3]

2 The model

2.1 Definition

The five dimensional anisotropic U(1) gauge model with two couplings, β and β', at finite temperature is defined as :

$$S_{gauge}^{5D} = \beta \sum_{x,1\leq\mu<\nu\leq3} (1 - Re(U_{\mu\nu}(x)) + \beta \sum_{x,1\leq\mu\leq3} (1 - Re(U_{\mu t}(x)) +$$
$$\beta' \sum_{x,1\leq\mu\leq3} (1 - Re(U_{\mu 5}(x)) + \beta' \sum_{x} (1 - Re(U_{t5}(x))) \tag{1}$$

---

[3]We recall that $T \equiv 1/L_t$ in lattice units.

where

$$
\begin{aligned}
U_{\mu\nu}(x) &= U_\mu(x)U_\nu(x+a_s\hat\mu)U_\mu^\dagger(x+a_s\hat\nu)U_\nu^\dagger(x) \\
U_{\mu t}(x) &= U_\mu(x)U_t(x+a_s\hat\mu)U_\mu^\dagger(x+a_t\hat t)U_t^\dagger(x) \\
U_{\mu 5}(x) &= U_\mu(x)U_5(x+a_s\hat\mu)U_\mu^\dagger(x+a_5\hat5)U_5^\dagger(x) \\
U_{t5}(x) &= U_t(x)U_5(x+a_t\hat t)U_t^\dagger(x+a_5\hat5)U_5^\dagger(x)
\end{aligned}
$$

are the plaquette variables defined on the 4d-subspaces $\{(\mu,\nu=1,2,3)$ - t$\}$ and planes containing an extra, fifth dimension (x_5). With an obvious noatation we call these plaquettes as P_s, P_{st}, P'_{s5} and P'_{t5}.

The link variables are defined as

$$
U_\mu(x) = e^{i\theta_\mu(x)}, \quad U_t(x) = e^{i\theta_t(x)} \text{ and } \quad U_5(x) = e^{i\theta_5(x)}
$$

Let us make the notation clear. The action is defined in an Euclidean lattice volume, namely $V = L_t \times L_s^3 \times L_5$ in lattice units. L_t is the compactified temporal dimension which is related to the temperature through the relationship

$$
T = \frac{1}{L_t a_t} \tag{2}
$$

We denote with a_t the lattice spacing, L_t is an integer number, $L_{s=1,2,3}$ are the usual "infinite" space dimensions and finally L_5 is an extra, fifth dimension, which we consider to be infinite and equal to L_s. We assume periodic bourdary conditions for the U(1) gauge field in all directions. The proclaimed anisotropy of the model has nothing to do with the "time" direction. In this model the lattice spacings a_s,a_t are equal. The anisotropy is introduced through the interaction along the extra direction. So, we have $a_s = a_t \equiv a$ and $a_5 \neq a$ where a_5 is the lattice spacing related to the extra dimension.

In our model the gauge couplings β and β' are generally independent from each other and the coordinates. The lattice spacing is determined from the value of the couplings β and β'. In some cases we can have a coordinate dependence and it is possible to relate them with extra fields, as in the brane model [2, 3, 17]. In terms of the continuum fields the link angles, θ_M, can be written as :

$$
\theta_M(x) = a_M \bar A_M(x)
$$

where $\bar A_M(x)$ are the gauge potentials [3, 8] and with M we denote $M = (t, \mu, 5)$. In the naïve continuum limit ($a, a_5 \to 0$) we define:

$$
\beta = \frac{a_5}{g_5^2} \quad \text{and} \quad \beta' = \frac{a^2}{g_5^2 a_5}
$$

where g_5 is the bare five-dimensional coupling constant for the gauge field. The resulting continuum action takes the standard form:

$$
S_{gauge} = \int d^5x \frac{1}{g_5^2}\overline{F}_{MN}^2 \, , \quad \overline{F}_{MN} = \partial_M\overline{A}_N - \partial_N\overline{A}_M.
$$

Note that g_5^2 has dimensions of length and is related to a characteristic scale for five dimensions. The previous expression does not exhibit any anisotropy at all. However, the results that we present below indicate that the anisotropy may survive in the continuum limit.

2.2 Observables

We now proceed to the introduction of the observables, i.e. the gauge invariant quantities which are used for the study of the model.

2.2.1 The helicity modulus

Among the quantities used to distinguish the various phases and the respective phase transitions in a statistical model the ones that attract the most attention are the so called order parameters. Their great significance comes from the fact that they display completely different behavior between the various phases. Their "thermal average" is zero on the one side of the transition and moves away from zero on the other side. For the case of a confining-Coulomb transition a quantity with the properties of an order parameter is the helicity modulus (**h.m**). It was first introduced in the context of lattice gauge theories by P.de Forcrand and M. Vettorazzo and it characterizes the responce of a system to an external flux. It is zero in a confining phase and nonzero in a coulombic one[13].

Let us consider our five dimensional system with $(L_\mu, L_\nu, L_\rho, L_t, L_5)$ and let us choose a particular orientation, for example, (μ, ν). Through the remaining orthogonal directions it is defined a stack of $L_\rho \times L_t \times L_5$ plaquettes parallel to the (μ, ν) orientation. In order to study the response of the system to an external static field we assume the presence of an external flux Φ through this stack of plaquettes. By a suitable choice of variable transformations we can spread the flux homogeneously over the parallel planes. In other words, we can add the constant value of $\Phi_P = \frac{\Phi}{L_\mu L_\nu}$ to each of the plaquettes of the given (μ, ν) orientation. Also we can impose an external flux by changing the boundary links using twisted boundary conditions instead of using pure periodic [13, 18]. The partition function, in the presence of the external flux, is:

$$Z(\Phi) = \int D\theta e^{-S(\theta;\Phi)} \qquad (3)$$

$$S(\theta; \Phi) = -\beta \sum_{(\mu\nu)planes} \cos(\theta_{\mu\nu} + \frac{\Phi}{L_\mu L_\nu}) - \beta \sum_{(\overline{\mu\nu})planes} \cos(\theta_{\overline{\mu\nu}})$$

$$-\beta \sum_{x,1\leq\mu\leq3} \cos(\theta_{\mu t}(x)) - \beta' \sum_{x,1\leq\mu\leq3} \cos(\theta_{\mu 5}(x))$$

$$-\beta' \sum_{x} \cos(\theta_{t5}(x)) \qquad (4)$$

6

where $\sum_{(\mu\nu)planes}$ is the sum over the plaquettes of the given orientation (μ, ν), containing the flux and $\sum_{(\overline{\mu\nu})planes}$ its complement, consisting of all the plaquettes that remained unchanged (plaquettes belonging to the other planes).

¿From the partition function we can obtain the flux dependent free energy

$$F(\Phi) = -\ln(Z(\Phi)) = -\ln\left(\int D\theta e^{-S(\theta;\Phi)}\right) \tag{5}$$

An important observation is that the partition function $Z(\Phi)$ of equation (3) and hence the flux free energy is clearly 2π periodic . So, the extra flux we impose on the system is defined only $\mod(2\pi)$.

In the confining phase the flux free energy $F(\Phi)$ is constant in the thermodynamic limit because the correlation length and the effect of the external flux through the twisted boundary links is exponentially decreasing. On the contrary, in the Coulomb phase we have an infinite correlation length, so the influence of the twisted boundary conditions is extended to the full extent of the system. As a result we have a nontrivial dependence of $F(\Phi)$ by the external flux Φ.

The helicity modulus is defined as

$$h(\beta) = \left.\frac{\partial^2 F(\Phi)}{\partial \Phi^2}\right|_{\Phi=0} \tag{6}$$

and it gives a measure of the curvature of the free energy profile around $\Phi = 0$. From the above equation and for various choices with respect to the orientation, due to the anisotropy of the model, we have:

$$h_s(\beta) = \frac{1}{(L_\mu L_\nu)^2}\left(\left\langle \sum_{P_s}(\beta\cos(\theta_{\mu\nu}))\right\rangle - \left\langle (\sum_{P_s}(\beta\sin(\theta_{\mu\nu})))^2 \right\rangle\right) \tag{7}$$

$$h_t(\beta) = \frac{1}{(L_\mu L_t)^2}\left(\left\langle \sum_{P_{st}}(\beta\cos(\theta_{\mu t}))\right\rangle - \left\langle (\sum_{P_{st}}(\beta\sin(\theta_{\mu t})))^2 \right\rangle\right) \tag{8}$$

$$h_{s5}(\beta') = \frac{1}{(L_\mu L_5)^2}\left(\left\langle \sum_{P'_{s5}}(\beta'\cos(\theta_{\mu 5}))\right\rangle - \left\langle (\sum_{P'_{s5}}(\beta'\sin(\theta_{\mu 5})))^2 \right\rangle\right) \tag{9}$$

$$h_{t5}(\beta') = \frac{1}{(L_t L_5)^2}\left(\left\langle \sum_{P'_{t5}}(\beta'\cos(\theta_{t5}))\right\rangle - \left\langle (\sum_{P'_{t5}}(\beta'\sin(\theta_{t5})))^2 \right\rangle\right) \tag{10}$$

Now, consider for the moment the classical limit $(\beta \to \infty)$ for the action (4) where all the fluctuations are suppressed. In this limit the flux is distributed equally over all the plaquettes of each plane and it does not change as we cross the parallel planes. If we expand the classical

7

action in powers of the flux, since in the thermodynamic limit the quantity $\frac{\Phi}{L_\mu L_\nu}$ is always small , we find:

$$S_{\text{classical}}(\Phi) = \frac{1}{2}\beta\Phi^2 \frac{V_{5D}}{(L_\mu L_\nu)^2} + \text{constant} \implies F_{\text{classical}}(\Phi) - F_{\text{classical}}(0) = \frac{1}{2}\beta\Phi^2 \frac{V_{5D}}{(L_\mu L_\nu)^2}$$

where $V_{5D} = L_\mu L_\nu L_\rho L_t L_5$ is the 5D lattice volume.

The above expression for the free energy, F, holds all the way up to the phase transition, where fluctuations are present, if one only replaces the bare coupling by a renormalized coupling, $\beta \to \beta_R(\beta)$ (for details see [18, 13]):

$$F_{[\text{finite } \beta]}(\Phi) - F_{[\text{finite } \beta]}(0) = \frac{\beta_R}{2}\Phi^2 \left(\frac{L_\rho L_t L_5}{L_\mu L_\nu} \right) \tag{11}$$

¿From the Eqs. (6) and (11) we have for the "spatial" h.m

$$h_s(\beta) \sim \beta_R L_t \tag{12}$$

and following the same steps, we can get the scaling relations for the remaining quantities:

$$h_t(\beta) \sim \beta_R \frac{L_\mu^2}{L_t} \tag{13}$$

$$h_{s5}(\beta') \sim \beta'_R L_t \tag{14}$$

$$h_{t5}(\beta') \sim \beta'_R \frac{L_\mu^2}{L_t} \tag{15}$$

Although the arguments presented above are based mainly on the classical approach, this is indeed the case in the Coulomb phase and the helicity moduli applied for the five dimensional system behave exactly as the above equations predict.

2.2.2 Polyakov loop (or Wilson line)

For the evaluation of the potential between a static quark-antiquark pair at zero temperature, the study of the ground state expectation value of the Wilson loop for large Euclidean times is needed. When the temperature is non zero ($L_t << L_s$ as opposed to the former case) the same information is obtained by using a different quantity which is the Polyakov loop or the Wilson line. It consists of the product of link variables along topologically non-trivial loops, winding around the time direction due to periodic conditions.

$$P_t(\vec{n}, n_5) = \prod_{n_t=1}^{L_t} U_t(\vec{n}, n_t, n_5)$$

$$P_t = \frac{1}{L_s^4} \sum_{(\vec{n}, n_5)} P_t(\vec{n}, n_5) \tag{16}$$

8

where $\{n\}\epsilon Z^5$ denotes a lattice site.

Physically, the expectation value of the Polyakov loop determines the free energy of a system with a single, static heavy quark, measured relative to the vacuum:

$$\langle|P_t|\rangle = e^{-L_t F_q} \tag{17}$$

where $|P|$ is the absolute value of P and $< \cdots >$ the statistical average value evaluated using the action of equation (1). The above relation holds even in the presence of finite mass quarks coupled to the gauge potential with the only difference that in that case the expectation value has to be calculated using the finite temperature action that includes the dynamical fermions.

The Polyakov loop is somewhat the world line of a static quark in a Wilson loop and that suggests that the free energy of a quark-antiquark pair located at $(\vec{n_1}, n_{5_1})$ and $(\vec{n_2}, n_{5_2})$ respectively is given by the correlation function of two such loops, with bases at the aforementioned points and having opposite orientations. Consequently we have:

$$\left\langle P_{t_1}(\vec{n_1}, n_{5_1}) P_{t_2}^\dagger(\vec{n_2}, n_{5_2}) \right\rangle = e^{-L_t F_{q\bar{q}}(\{\vec{n_1}, n_{5_1}\};\{\vec{n_2}, n_{5_2}\})} \tag{18}$$

keeping L_t constant.

For large distance separation of the quark-antiquark pair and assuming that the correlation functions satisfy clustering, the above expression reduces to

$$\left\langle P_{t_1}(\vec{n_1}, n_{5_1}) P_{t_2}^\dagger(\vec{n_2}, n_{5_2}) \right\rangle \to |\langle P_t \rangle|^2 \text{ for } |\hat{R}| \to \infty \quad (\text{where } \hat{R} = \{\vec{n_1}, n_{5_1}\} - \{\vec{n_2}, n_{5_2}\}) \tag{19}$$

which is just the self-energy of two isolated quarks.

In the confinement phase the correlation function of the Polyakov loop decays exponentially for large distances:

$$\left\langle P_t(0) P_t^\dagger(\hat{R}) \right\rangle \sim e^{-L_t \sigma |\hat{R}|} \tag{20}$$

giving a linear potential with string tension σ and $F_{q\bar{q}} \simeq \sigma |\hat{R}|$.

The flux free energy $F_{q\bar{q}}$ increases, in general, for large separation of the quarks in the confining phase, giving eventually $< |P_t| >= 0$ and $F_{q\bar{q}} = \infty$ in the thermodynamic limit. We interpret $< |P_t| >= 0$ as a signal for confinement. If we have $< |P_t| > \neq 0$, then the free energy of the static quark-antiquark pair tends to a constant value, for large separation of the heavy charges, as shown in Eqs. (18) and (19), and this is a signal for deconfinement. In other words, the expectation value of the temporal Polyakov loop serves as an order parameter in finite temperature gauge theories.

3 Three limitting cases

3.1 The zero temperature case

The five dimensional anisotropic U(1) gauge model, at zero temperature, was first introduced by Fu and Nielsen [1] as an attempt to offer an alternative way to achieve dimensional reduction. Since then many numerical investigations of the model have been made [15, 16]. As we have already noted in the Introduction, the interest in this comes from the fact that the anisotropy of the model produces a new phase, the so called layer phase, which can serve as a mechanism for gauge field localization on a brane. We can induce this anisotropy to the gauge coupling using, for example, the Randall-Sundrum metric background in five dimensions. The effect of the warp factor from the RS background or a general anti-de-Sitter (AdS_5) background on the U(1) gauge theory is to provide the gauge theory with a different gauge coupling in the fifth direction([3]).

In Fig. 1 we present the phase diagram of the theory. It consists of three distinct phases. For large values of β and β' the model lies in a Coulomb phase (**C**) on the 5-D space. Now, if one keeps β constant and bigger than one and at the same time lets decrease β', one will eventually come across the new phase, the layer phase (**L**), where the forces in four dimensions will still be Coulomb-like but in the fifth dimension the confinement is present. For small values of β and β' the force is confining in all five directions and the corresponding phase is the Strong phase (**S**). The properties of the three phases can become more transparent in terms of two test charges.
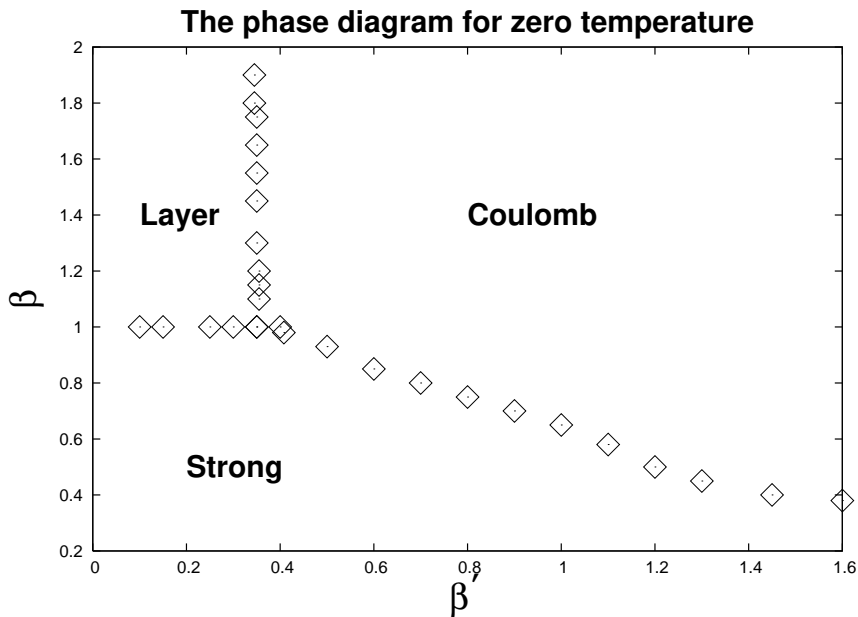

Figure 1: The phase diagram for the 5D anisotropic U(1) gauge model at zero temperature. Three phases are present: Strong confining phase, 5D Coulomb phase and the Layer phase.

In the Coulomb phase the force between two heavy charges is 5D Coulomb-like, and becomes the exact five dimensional Coulomb law in the diagonal line, defined by $\beta = \beta'$ for which no anisotropy appears (for a numerical investigation see [4]). The completely opposite picture emerges in the Strong phase. There the force is confining in all five directions giving infinite energy for the separation of the test charges in any direction. Now, two test charges in the layer phase will experience a Coulomb force in the four dimensional layers, with the coupling given by the four-dimensional coupling β; there are strong indications of the similarity with the usual 4D Coulomb law (see [4] for details), while along the fifth direction the test charges will experience a strong force as the corresponding coupling β' takes small values. This means that charged particles in the layer phase will mainly run only along a layer since in an attempt to leave the layer in which they belong they will be driven back by a linear potential, analogous to the one responsible for the quark confinement. This is the mechanism on which the gauge field localization scheme is based.

Now we would like to sketch the three phases in terms of the helicity modulus. In the zero temperature case ($L_t = L_s \equiv L_5$) we are left with only two possible choices. Instead of the Eqs. (7)-(10) we have:

$$h_S(\beta) = \frac{1}{(L_\mu L_\nu)^2} \left(\left\langle \sum_P (\beta \cos(\theta_{\mu\nu})) \right\rangle - \left\langle (\sum_P (\beta \sin(\theta_{\mu\nu})))^2 \right\rangle \right) \tag{21}$$

$$h_5(\beta') = \frac{1}{(L_\mu L_5)^2} \left(\left\langle \sum_{P'} (\beta' \cos(\theta_{\mu 5})) \right\rangle - \left\langle (\sum_{P'} (\beta' \sin(\theta_{\mu 5})))^2 \right\rangle \right) \tag{22}$$

The first one, $h_S(\beta)$, is used to probe the response of the system to an external flux in the spatial planes (belonging to a 4d layer) while the second one, $h_5(\beta')$, is used in a similar way for the planes containing the extra, transverse direction.

(i) In the Strong phase (keeping β' constant) the space-like helicity modulus vanishes (which is a clear signal of confinement); as we approach and eventually pass the phase boundary it becomes non-zero in the layer phase with a value that approaches 1 as β increases further. On the other hand, the transverse h.m, $h_T(\beta')$, remains zero throughout the transition since both phases exhibit confinement in the fifth direction.

(ii) For the transition between the 5D Coulomb phase and the layer phase, $h_S(\beta)$ retains a value close to 1 for all values of β', since the four dimensional layers experience already a 4d Coulomb-like phase, while $h_T(\beta')$ vanishes for the layer phase; as the system crosses the critical point and enters the Coulomb phase it grows towards 1 as β' increases further [4, 15].

3.2   The $\beta' = 0$ case

On the axis defined by $\beta' = 0$ we consider the four-dimensional U(1) model. In this section our intention is to strengthen the arguments given in references [13]. We present numerical results

showing that we have a Coulomb phase only for T=0, in accordance with Fig. 12 of [13]. Our findings contradict the ones of ref. [12] that stipulates the existence of a Coulomb phase for $L_t \geq 4$ and $\beta \geq \beta_c$. The numerical results presented below show that we have a spatial confinement phase when the spatial lattice size L_s gets big enough, compared to the temporal size L_t $(L_s \gtrsim 4L_t)$.

This behavior can be understood, following closely the ref. [13], using simple theoretical arguments. In order to have $h_s(\beta) \sim 0$, one must have at least two monopole loops (far apart) winding around the time direction with opposite orientations. A non contractible time-like monopole loop can, in principle, disorder all the spatial planes in the lattice. The probability to have one such loop passing through a given lattice site is, roughly, $e^{-m_{\mathrm{mon}}(\beta)L_t}$, where $m_{\mathrm{mon}}(\beta)$ is the monopole mass. So the condition to achieve a probability of order 1 for a system to containing one (or two) wrapping monopole loops, is:

$$L_s^3 \times e^{-m_{\mathrm{mon}}(\beta)L_t} \sim 1 \Longrightarrow L_s \sim e^{\frac{L_t}{3}m_{mon}(\beta))} \Longrightarrow L_s \sim e^{\frac{L_t}{3}c\beta} \tag{23}$$

since $m_{\mathrm{mon}}(\beta)$ is of order β. Now, starting from the above equation we can make two statements. First, it predicts a pseudocritical coupling $\beta_c \sim \log(L_s)$ which was verified by our measurements and second, that as we go to smaller temperatures (bigger L_t), for sufficiently large L_s Eq. (23) is satisfied; hence the spatial planes becomes completely disorder and the Coulomb phase disappears.
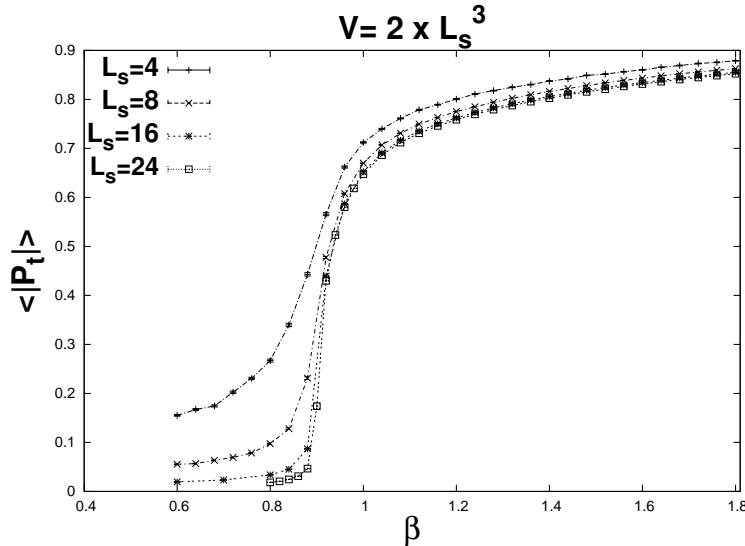

Figure 2: The mean value $< |P_t| >$ of the temporal Polyakov loop for $\beta' = 0$ and temporal size $L_t = 2$. $< |P_t| >$ goes to zero in the confining phase for $L_s \to \infty$. In the deconfinement phase $(\beta > \beta_c(L_t))$ $< |P_t| >$ is non-zero, approaching the value of one as β increases

In Fig. 2 we show the mean value of the temporal Polyakov loop $P_t(\beta)$ for $L_t = 2$. There

is an obvious continuous phase transition from the confining phase ($\beta \leq \beta_c \simeq 0.90$), where $< |P_t| >$ is zero, to the deconfining phase where $< |P_t| >$ approaches the value of one. In the confining phase the free energy of a single static charge, relative to the vacuum, goes to infinity with L_s while it gets a positive value in the deconfining phase which vanishes as β increases. The mean value of the temporal Polyakov loop remains always non zero in the finite temperature phase as we switch on β'. This is the case presented in section 4. However this order parameter does not help us to characterize further the nature of the different phases. We arrived at the conclusion that the helicity modulus is a more promising quantity to study in detail the phase diagram.
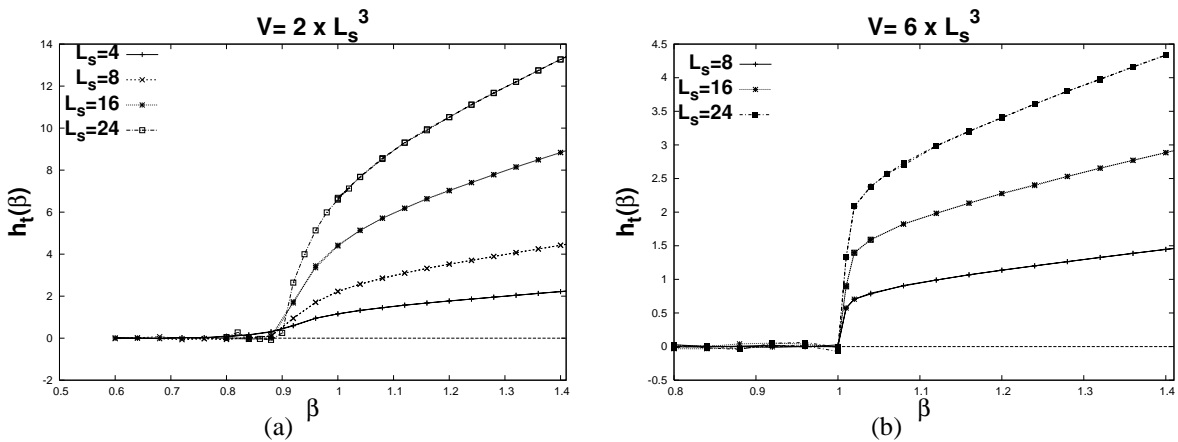

Figure 3: The temporal helicity modulus h_t for $L_t = 2$ (a) and $L_t = 6$ (b) and $\beta' = 0$. Results from three different volumes are present. The value of h_t increases with L_s in the deconfine region, for β bigger than a critical value, again with accordance with the scaling predictions of section (2.2.1). The transition for $L_t = 2$ is continuous, as opposed to the $L_t = 6$ case, where we have a discontinuous behavior.

In figure 3 we present our results for the temporal helicity modulus $h_t(\beta)$ for two different "temperatures" $L_t = 2$ and $L_t = 6$. The temporal h.m is zero in the confining phase for $\beta < \beta_c(L_t)$ and non-zero for $\beta \geq \beta_c(L_t)$ in the deconfining phase, indicating coulombic behavior. The signal for $h_t(\beta)$ in the deconfining phase ($\beta \geq \beta_c$) is being enhanced with increasing L_s, following the scaling relation $h_t \sim \frac{L_s}{L_t}$. The transition point has only a weak dependence from the lattice volume showing convergence to a critical value $\beta_c(L_t)$ with L_s. We see that $\beta_c(L_t)$ tends to smaller values as L_t decreases.[4] Another noticeable difference is the behavior of h_t in the critical region. For $L_t = 2$, $h_t(\beta)$ goes continuously to zero when β approaches β_c from above. For $L_t = 6$, on the other hand, the h_t has an obvious discontinuity as β approaches β_c

---

[4] $\beta_c(L_t = 2) = 0.9008(3)$, $\beta_c(L_t = 4) = 1.00340(1)$ and $\beta_c(L_t = 6) = 1.0094491(1)$. The results are taken from ref. [13].

and the volume increases. This behavior indicates a different order for the phase transition, a second order phase transition for $L_t = 2$ and a first order for $L_t = 6$ (for details see ref. [13]).

In Fig. 4 we show the spatial helicity modulus $h_s(\beta)$ for $L_t = 2$ and spatial lattice sizes $L_s = 4, 8, 16$ and 24. The spatial helicity modulus is zero for β smaller than a critical value $\beta_c(L_s)$ that depends strongly on L_s. We shall refer from now on to $\beta_c(L_s)$ as the pseudocritical value, to distinguish it from the real critical value of β that comes from the temporal helicity modulus $h_t(\beta)$. For $\beta \geq \beta_c(L_s)$, h_s takes non-zero values, increasing linearly as β takes bigger values . On the other side, the magnitude of this quantity decreases according to the ratio $\sim \frac{L_t}{L_s}$, as we increase L_s and tends to zero for $L_s \to \infty$. The pseudocritical value $\beta_c(L_s)$ increases with L_s as $\log(L_s)$ [13] and the ratio $\frac{\beta_c(L_s)}{\log(L_s)}$ tends to the value 0.5 for $L_s \geq 16$. In this way $\beta_c(L_s)$ goes to infinity when $L_s \to \infty$. As a result the spatial h.m is always zero in the infinite volume limit and as a consequence we have a spatial confining phase.
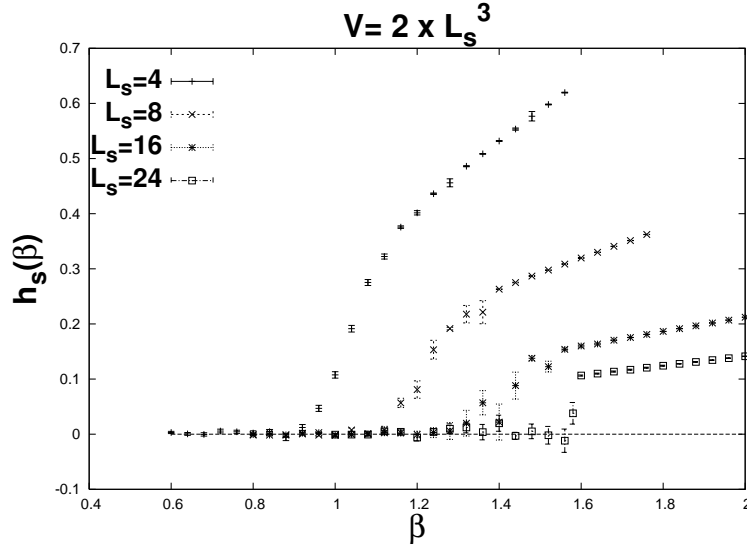

Figure 4: The spatial helicity modulus h_s for $L_t = 2$ and $\beta' = 0$, versus the four dimensional coupling β. The pseudo critical value of β increases very fast, towards an infinite value, as the spatial lattice size L_s increases. The shift of the transition region to bigger values of β is obvious even in the smaller volumes.

Finally we study the spatial helicity modulus for $L_t = 4$ and $L_t = 6$. The results are shown in Figs. 5(a)($L_t = 4$) and 5(b)($L_t = 6$). We have, in general, the same situation as for $L_t = 2$. There is a pseudo-critical value of β that moves to larger values as L_s increases showing a strong dependence on L_t. The signal for $L_t = 4$ is clear only for $L_s \geq 16$. For $L_t = 6$ it seems that $L_s = 16$ is not enough but for $L_s \geq 24$ we get a clear displacement of $\beta_c(L_s)$ to the right. In the region $\beta \leq \beta_c(L_s)$ the spatial helicity modulus is zero (confining region). For $\beta > \beta_c$ the spatial h.m scales with $\sim \frac{L_t}{L_s}$ and tends to zero for $L_s \to \infty$. If we examine the $L_t = 8$ case for example, we would probably need volumes bigger than 8×32^3 in order to get a clear picture

of the behavior of the system. From the previous observations we can say that $h_s(\beta)$ is zero for every value of β in the infinite volume limit, and consequently, we have spatial confinement for all temperatures different from zero.

We conclude that the phase diagram on the β, $T = \frac{1}{L_t}$ plane has three phases: a confining phase for $\beta < \beta_c(L_t)$, a temporal Coulomb - spatial confining phase for $\beta > \beta_c(L_t)$ [5] and the pure Coulomb phase for $L_t \to \infty$ and $\beta > \beta_c$ [13, 14].
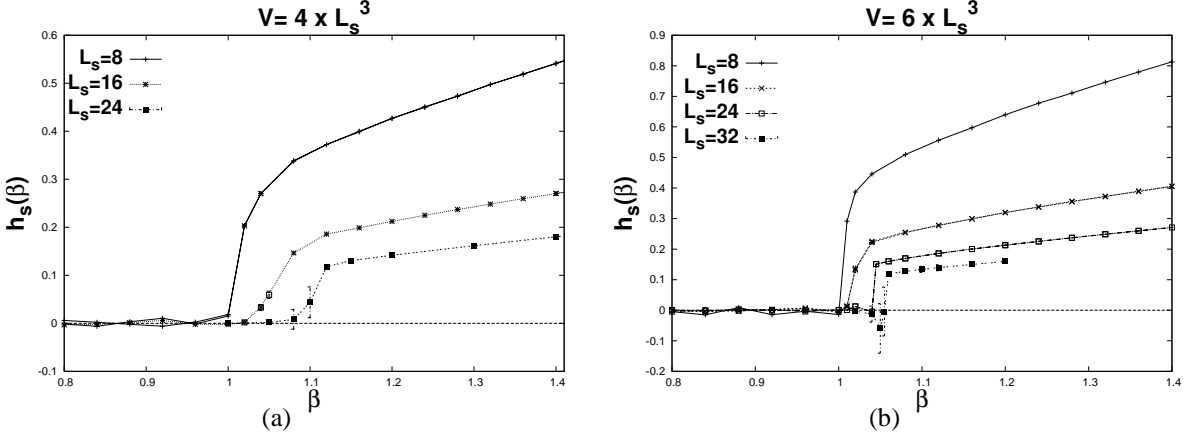

Figure 5: In figures (a) and (b) we present the spatial h.m (h_s) for $\beta' = 0$ and different temporal sizes, $L_t = 4$ and $L_t = 6$, for a variety of spatial volumes. The size of h_s decreases with L_s when β takes values bigger than the pseudo critical value, as predicted in section (2.2.1). The transition region moves clearly to the right as the volume increases, in agreement with the $L_t = 2$ behavior.

3.3 $L_t = 1$

In this case the temporal link is a Polyakov loop by itself and of course it is a gauge invariant quantity. The temporal plaquette becomes:

$$\theta_{\mu t}(x) = \theta_\mu(x) + \theta_t(x + \hat{\mu}) - \theta_\mu(x) - \theta_t(x)$$

The two spatial links cancel each other, so in the U(1) case we get:

$$\theta_{\mu t}(x) = \theta_t(x + \hat{\mu}) - \theta_t(x)$$

The contribution to the action is:

$$S_t = -\beta \sum_{x,1\leq\mu\leq3} \cos(\theta_t(x + \hat{\mu}) - \theta_t(x)) \tag{24}$$

---

[5]This phase is usually called deconfining phase.

15

The same applies for the "temporal-transverse" plaquettes and following the same steps as above we find that their contribution to the action is :

$$S_{t'} = -\beta' \sum_x \cos(\theta_t(x + \hat{5}) - \theta_t(x))$$ (25)

From the above equations it can be observed that the temporal plaquettes decouple from the space and transverse ones. Equations (24) and (25) describe a 4D **XY** model with anisotropic couplings (β, β'). The three spatial links and the fifth, transverse link form a separate four dimensional anisotropic U(1) gauge theory with two couplings, β and β'. As a result the partition function of the model reduces to:

$$Z_{(\mathbf{L_t=1})} = Z_{\text{anisotropic 4D-XY}} \times Z_{\text{anisotropic 4D-U(1)}}$$ (26)

and it describes two independent lattice field theories.

The anisotropic $4D - \mathbf{XY}$ model, for $\beta' = 0$, reduces to the three dimensional **XY** model which has a second order phase transition for $\beta = 0.4542$ [19]. The phase transition line continues to the (β, β') plane for smaller values of β as β' increases and the critical value of β seems to tend asymptotically to the value of 0.1 as β' goes to infinity. [6]

The 4D gauge model for $\beta' = 0$ reduces to a three dimensional U(1) gauge theory which is always in the confining phase. In the (β, β') plane we have a critical line which separates the strong confining phase from the four dimensional Coulomb phase. If we move along the diagonal, for example, where $\beta = \beta'$, we get the usual weak first order phase transition for $\beta = \beta' = 1.001113$ [20, 15].

The above discussion can be summarized in the three dimensional plot of Fig. 6 . The vertical axis is for the temperature given in terms of the discrete variable L_t. The upper plane for $L_t = 1$ corresponds to "infinite" temperature while the lower plane for $L_t = L_5 = L_s$ corresponds to the zero temperature case.

4 Study of the phase diagram for $\mathbf{L_t} = 2$.

In five dimensions the phase diagram at zero temperature is given in Fig. 1. [7] For $0 \leq \beta' < 0.40$ and $\beta \approx 1$. there is a critical horizontal line in the phase diagram separating the 5D strong confining phase from the layer phase. For $\beta > 1$ and $\beta' \simeq 0.35$ there is a critical vertical line that separates the layer from the 5D Coulomb phase. Our intention in this section is to explore the effects of finite temperature on our system and the most important, the feasibility (if any) of a layer phase, through the study of the changes in the aforementioned phase line boundaries

---

[6]For example, for the 4D **XY** model the critical value is at $\beta = \beta' = 0.29(1)$ (see Fig. 6).
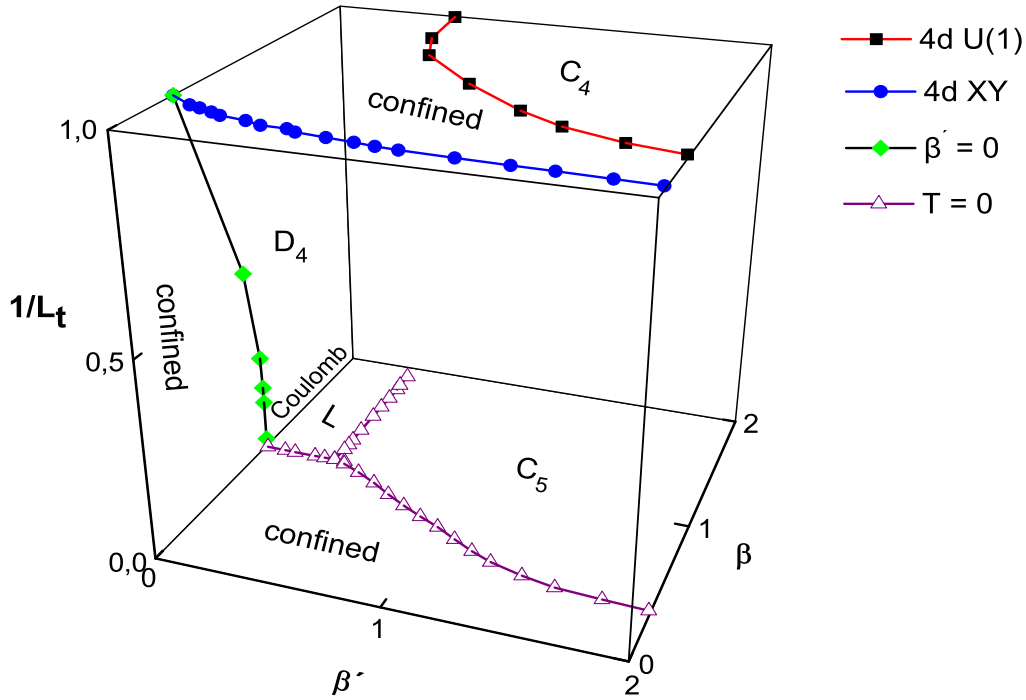[7]Lower plane ($1/L_t = 0.0$), see Fig. 6.

Figure 6: Three dimensional phase diagram of the model, the vertical axis ($1/L_t$) represents the temperature. We present the critical curves for the three limiting cases. C_4 and C_5 are the four dimensional and the five dimensional Coulomb phases respectively. L stands for the layer phase at zero temperature. D_4 is the temporal Coulomb - spatial confining phase for $\beta' = 0$.

and the phases themselves. To that end we move, first, on the line $\beta' = 0.20$ in order to study the strong-layer phase transition at finite T; we know that for $\beta' = 0$ (subsection 3.2) there is phase transition for $\beta \simeq 0.90$. Second, we move along the line $\beta = 1.10$, in order to study the layer-Coulomb phase transition at finite temperature.[8] As we will explain in section 4.2 and using the Figs. 4 and 7 in order to have a clear picture of the behavior of the system for bigger values of β we need even bigger five dimensional volumes than those that we can presently achieve.

Using the results presented in the two following sections we can argue that the layer phase disappears for $L_t = 2$ and becomes a deconfined phase with new properties which will be described below. We can also generalize the arguments and say that there is no layer phase in finite temperature for any temperature different from zero. The existence of the layer phase is based strongly on the existence of the Coulomb phase for $\beta' = 0$. However there is no Coulomb phase for $\beta' = 0$ at $T \neq 0$ as it is argued in ref. [13]. We also confirm this result (see subsection 3.2).

---

[8]We refer to the case of the plane (β, β') at $1/L_t = 0.5$ in Fig. 6.

4.1 Moving along the line $\beta^{'}$=0.20

We begin the investigation of the 5D anisotropic pure U(1) gauge model at finite temperature with what used to be called as a 5D strong-layer phase transition at zero temperature (Fig. 1). We utilize the helicity modulus $h_s(\beta), h_t(\beta)$ in order to bring out the features of the transition and compare them with the T=0 and $\beta^{'} = 0$ cases. As it is shown in Fig. 3 the first deviation from the zero temperature case comes from the fact that now, the transition line boundary between the two phases, is found at a lower value of $\beta = 0.90$ in contrast with the value of $\beta = 1.001113$ for $T = 0$ case. Another observation is that the values obtained here concerning $h_t(\beta)$ are of the same order of magnitude as the ones, for the $\beta^{'} = 0$ case; the only difference is the slight movement of the critical region to a value between 0.85 and 0.90.

Moving now to a discussion of Fig. 7 and the spatial helicity modulus $h_s(\beta)$ we encounter many similarities with the results of subsection 3.2 :

i) There is a pseudocritical value $\beta_c(L_s)$ for each lattice size, with h_s equal to zero for $\beta \leq \beta_c(L_s)$, signal of spatial confinement. For $\beta > \beta_c(L_s)$ the spatial helicity modulus h_s increases with β, as one would expect from a Coulomb phase. But the transition point moves to higher and higher values of β as the spatial extent of the lattice (L_s) grows. What we see here is only a finite size effect that ceases to exist in the thermodynamic $L_s \to \infty$ limit.

ii) The magnitude of $h_s(\beta)$, calculated on a single 4d layer, decreases with L_s for the same value of β for $\beta > \beta_c(L_s)$, following the ratio $\sim \frac{1}{L_s}$. So we expect, as in the 4d case for $\beta^{'} = 0$, that the spatial helicity modulus tends to zero for all values of β as $L_s \to \infty$ (indicating spatial confinement); the phase transition to a Coulomb phase disappears together with the layer phase in the infinite volume limit. We mention also that the spatial-transverse helicity modulus $(h_{s5}(\beta))$ remains zero throughout the transition.
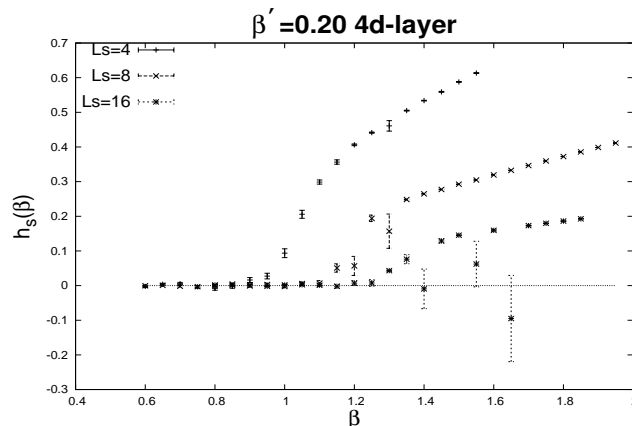

Figure 7: The spatial helicity modulus h_s is strictly zero for each volume $V = 2 \times L_s^4$ until the pseudo-critical value $\beta_c(L_s)$ is approached. For $\beta > \beta_c(L_s)$ the h_s tends to zero as $\frac{1}{L_s}$ for constant β.

18

In Fig. 8(a) we present the temporal helicity modulus h_t; also, in Fig. 8(b) we present the temporal-transverse helicity modulus h_{t5} versus β, for three different volumes. The two quantities have the same behavior: both take values equal to zero for $\beta \leq 0.85$ and non-zero for $\beta > 0.85$ and they increase with the lattice size L_s, indicating a coulombic behavior in the temporal direction. We also note that the Polyakov loop in the temporal direction, a result not shown here, is zero for β smaller than a critical value ($\beta_c \simeq 0.85$) and tends to one for $\beta > \beta_c$. The transition, for the three quantities h_t, h_{t5} and $< |P_t| >$, concerning the strong confining phase ($\beta \leq 0.85$) to the deconfining phase ($\beta > 0.85$) is a continuous one . Although we do not analyze further the order of this phase transition we may guess that it may not be the case of a first order phase transition.

All of the results obtained so far advocate to the disappearance of the layer phase at finite temperature. The layer gives its place to a phase showing a confining behavior in the 4d subspaces (formed by the three spatial coordinates and the transverse one) and a coulombic behavior along the temporal direction.
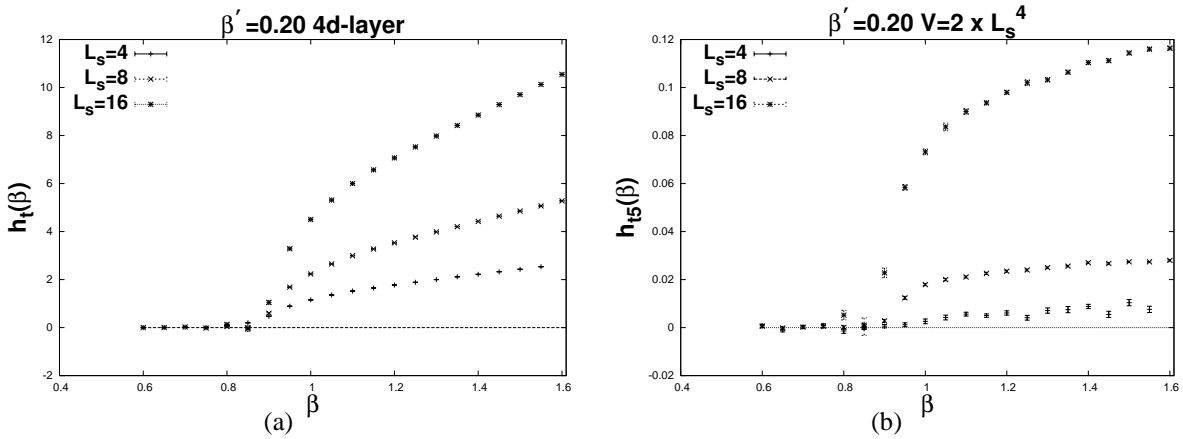

Figure 8: The temporal helicity modulus h_t (a) and the temporal-transverse helicity modulus h_{t5} (b) for $L_t = 2$ and $\beta' = 0.20$ versus β. The h_t is evaluated on the 4d-subspaces ($L_t \times L_s^3$) and scales as L_s for $\beta > \beta_c$. The h_{t5} is evaluated on the whole lattice and scales as L_s^2 for $\beta > \beta_c$.

4.2 Moving along the line $\beta = 1.10$

As we have seen in the previous sections the system undergoes a continuous phase transition from the strong, confining phase, to a new phase. The transition point for $\beta' = 0$ is shown to be $\beta_c \simeq 0.90$ and for $\beta' = 0.20$ it is slightly smaller being in the interval $0.85 \leq \beta_c < 0.90$ region. In order to study the nature and the extent of the new phase, we choose to keep β fixed at the value of 1.10 and let β' to vary. In Figs. 9(a) and 9(b) we present the spatial helicity modulus

19

$h_s(\beta')$ and the spatial-transverse helicity modulus $h_{s5}(\beta')$ for three values of the volume. The h_s and h_{s5} are zero, within the statistical error, for β' smaller than 0.445 signaling disordering in the spatial and transverse directions. This phase is the continuation of the $\beta' = 0$ phase to non zero values of β'. The 3d U(1) theory obtained through dimensional reduction for $\beta' = 0$, is extended (for $0 \leq \beta' \leq 0.445$) to a 4d dimensionally reduced U(1) theory in the confining phase. We observe that the layer phase, consisting of a combination of 4d Coulomb phase and confinement in the extra dimension, becomes a deconfined phase.

There is a critical region defined in the interval $(0.445 \leq \beta' \leq 0.450)$ in which a finite discontinuity in both quantities (h_s, h_{s5}) is shown up . For $\beta' > \beta'_c$ the spatial helicity modulus is non zero and almost constant which is a characteristic of a Coulomb phase. The value of $h_{s5}(\beta')$ increases linearly with β', following the lattice weak coupling expansion, approaching $h_s(\beta')$ as $\beta' \to \beta$. The values of h_s and h_{s5} in Fig. 9 are divided by L_t and are independent of the spatial lattice size L_s. The spatial helicity modulus gives the renormalized coupling $\beta_R = \frac{1}{e_R^2}$ of the 5D U(1) theory in the Coulomb phase which is fixed by the value of $\beta = 1.10$[4].

The temporal and the temporal-transverse helicity modulus (not shown here), remain non zero and increase with β'. Also the temporal Polyakov loop is non zero which is a signal of a finite temperature phase.
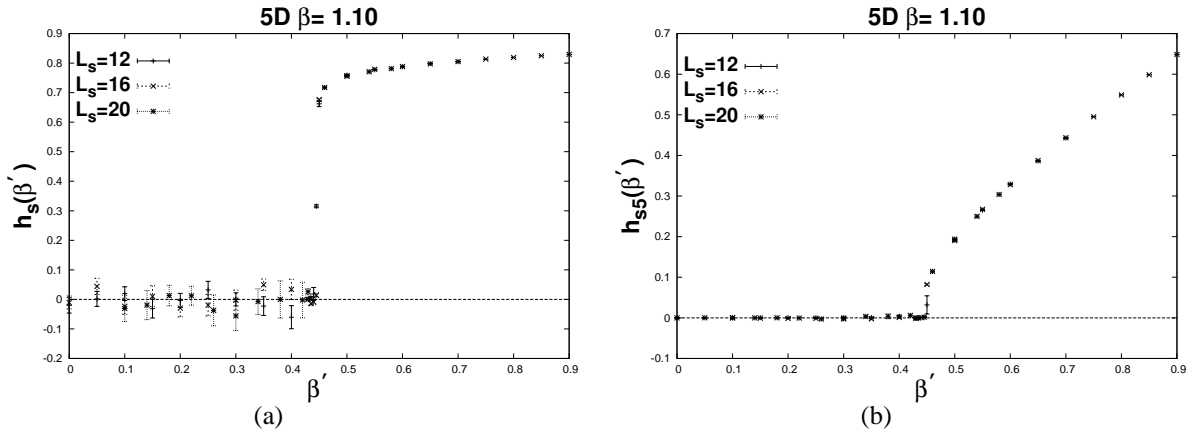

Figure 9: The spatial helicity modulus (a) and the spatial-transverse helicity modulus (b) as a function of β', measured for the temporal lattice size $L_t = 2$. The critical value of β' remains constant with the lattice volume.

By close inspection of Fig. 4 ($\beta' = 0$) and Fig. 7 ($\beta' = 0.20$), it becomes obvious that for a constant value of β the spatial helicity modulus is non-zero for some of the volumes that we used and it vanishes as the spatial volume increases beyond a definite value. For $\beta = 1.10$, for example, the lattice size $L_s = 16$ is enough to show the correct thermodynamic limit behavior. If we move to larger values of β, like $\beta = 1.40$, we have to use a spatial size of the order $L_s \geq 24$ in order to find the correct behavior. This is beyond our current computer capabilities.

20

In Fig. 10 we sketch, roughly, the phase diagram for $L_t = 2$ in the (β, β') plane. There are three phases with different behavior of the observables we used:

1. 5D confining phase with: $P_t = 0$, $h_t = 0$, $h_{t5} = h_{s5} = 0$ and $h_s = 0$

2. Finite temperature 5D Coulomb phase: $P_t \neq 0$, $\quad h_t, h_s, h_{t5}$ and $h_{s5} \neq 0$

3. Dimensionally reduced 4d confining phase-temporal Coulomb $P_t \neq 0$, $\quad h_t \neq 0$, $h_{t5} \neq 0$ and $h_s, h_{s5} = 0$
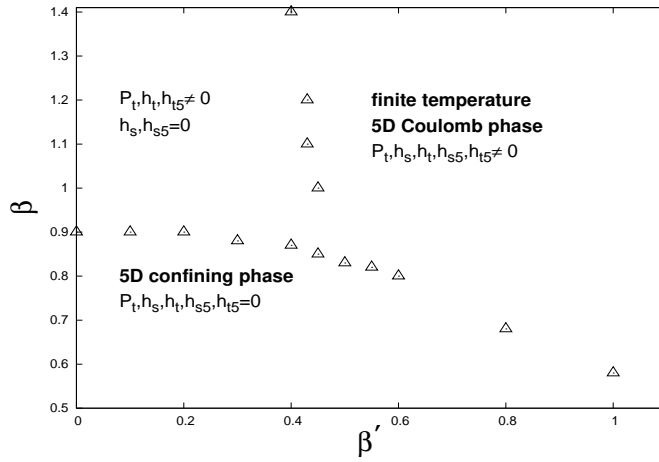

Figure 10: A rough sketch for the phase diagram of the model for $L_t = 2$. There are three different phases, a 5D confining phase, a 5D Coulomb phase in finite temperature and a new one characterized as temporal Coulomb-4d confining.

From the discussion in section 3.2 for $\beta' = 0$ we argue that the critical temperature for the appearance of the phase diagram of Fig. 10 it is the zero temperature. The reason is that the layer phase strongly depends on the existence of the phase transition in the Coulomb phase for $\beta' = 0$. All the results we have presented in section 3.2 for $T > 0$ and $\beta' = 0$ point to a 3d confining phase, in the infinite volume limit, for β larger than a critical value $\beta_c(L_t)$. A Coulomb phase does not seem to be the case. From this analysis we conclude that the phase diagram presented in Fig. 10 is reproduced for every temperature bigger than zero. Especially for $\beta > \beta_c(L_t)$ and $0 < \beta' < \beta'_c(L_t)$ we have a 4d confining-temporal coulombic phase instead of a layer phase. Two charges are not anymore localized (confined) on a three dimensional subspace (brane) but the temperature gives the possibility of having interactions between the neighbor three dimensional subspaces. It seems that there are two characteristic correlation lengths in this deconfining phase. The correlation length given by the spatial string tension and a second one characterising the thickness of the brane given by the interaction in the transverse direction and the temperature. We did not study quantitatively these two correlation lengths at

finite temperature but we may easily see from the Fig. 6 what happens in two limiting cases. For $L_t = 1$ (infinite temperature) we have a 4d U(1) gauge theory in the strong confining phase and the two correlation lengths are indistinguishable and approach each other. For the zero temperature case on the other hand, there is no spatial string tension; we get a massless photon on the branes. Note that in this case the branes are characterized by zero thickness. In between these two limiting cases we expect a continuous change in the behavior depending strongly on the temperature.

5   Discussion

The extra dimensional models, like the brane models, are well studied mainly in the zero temperature case. But if we imagine that our brane world is a part of the Universe history then a study of the brane models at high temperature is required. In this paper we tried to do a first approach to this open problem, namely the behavior of brane models in high temperature (though neglecting the gravity effects). We believe that our toy model of five dimensional U(1) anisotropic lattice gauge theory has all the required essential characteristics. This model has a very rich phase diagram with respect to the temperature (see the discussion in Sections 3 and 4) summarized in Figures 6 and 10.

Concluding we could note that the layer phase for zero temperature (with a massless photon on the brane and confinement in the extra dimensions) gives its place to a deconfined phase at non-zero temperature. In this phase the three spatial dimensions and the transverse one form a 4d subspace with confining properties, while the temporal direction shows a coulombic behavior.

6   Acknowledgments

References

[1] Y. K. Fu and H. B. Nielsen, Nucl. Phys. B **236** (1984) 167.

[2] L. Randall and R. Sundrum, Phys. Rev. Lett. **83**, 4690 (1999) [arXiv:hep-th/9906064];
     L. Randall and R. Sundrum, Phys. Rev. Lett. **83**, 3370 (1999) [arXiv:hep-ph/9905221].

[3] P. Dimopoulos, K. Farakos, A. Kehagias and G. Koutsoumbas, Nucl. Phys. B **617**, 237 (2001) [arXiv:hep-th/0007079].

[4] K. Farakos and S. Vrentzos, Phys. Rev. D **77**, 094511 (2008) [arXiv:0801.3722 [hep-lat]].

[5] G. R. Dvali and M. A. Shifman, Phys. Lett. B **396** (1997) 64 [Erratum-ibid. B **407** (1997) 452] [arXiv:hep-th/9612128].

[6] K. Farakos and P. Pasipoularides, Phys. Lett. B **621**, 224 (2005) [arXiv:hep-th/0504014]; K. Farakos and P. Pasipoularides, Phys. Rev. D **73**, 084012 (2006) [arXiv:hep-th/0602200]; K. Farakos and P. Pasipoularides, Phys. Rev. D **75**, 024018 (2007) [arXiv:hep-th/0610010]. P. Pasipoularides and K. Farakos, J. Phys. Conf. Ser. **68** (2007) 012041.

[7] L. X. Huang, T. L. Chen and Y. K. Fu, Phys. Lett. B **329**, 175 (1994).

[8] P. Dimopoulos, K. Farakos, C. P. Korthals-Altes, G. Koutsoumbas and S. Nicolis, JHEP **0102**, 005 (2001) [arXiv:hep-lat/0012028].

[9] P. Dimopoulos and K. Farakos, Phys. Rev. D **70** (2004) 045005 [arXiv:hep-ph/0404288]; P. Dimopoulos, K. Farakos and G. Koutsoumbas, Phys. Rev. D **65** (2002) 074505 [arXiv:hep-lat/0111047]; P. Dimopoulos, K. Farakos and S. Nicolis, Eur. Phys. J. C **24** (2002) 287 [arXiv:hep-lat/0105014].

[10] T. A. DeGrand and D. Toussaint, Phys. Rev. D **22**, 2478 (1980).

[11] M. N. Chernodub, E. M. Ilgenfritz and A. Schiller, Phys. Rev. D **64**, 054507 (2001) [arXiv:hep-lat/0105021]; M. N. Chernodub, E. M. Ilgenfritz and A. Schiller, Nucl. Phys. Proc. Suppl. **106**, 703 (2002) [arXiv:hep-lat/0110038].

[12] B. A. Berg and A. Bazavov, Phys. Rev. D **74**, 094502 (2006) [arXiv:hep-lat/0605019]; B. A. Berg and A. Bazavov, PoS **LAT2006**, 061 (2006) [arXiv:hep-lat/0609006].

[13] M. Vettorazzo and P. de Forcrand, Nucl. Phys. B **686**, 85 (2004) [arXiv:hep-lat/0311006]; M. Vettorazzo and P. de Forcrand, Nucl. Phys. Proc. Suppl. **129**, 739 (2004) [arXiv:hep-lat/0311007]; M. Vettorazzo and P. de Forcrand, Phys. Lett. B **604**, 82 (2004) [arXiv:hep-lat/0409135].

[14] C. Borgs, Nucl. Phys. B **261** (1985) 455.

[15] P. Dimopoulos, K. Farakos and S. Vrentzos, Phys. Rev. D **74**, 094506 (2006) [arXiv:hep-lat/0607033].

[16] A. Hulsebos, C. P. Korthals-Altes and S. Nicolis, Nucl. Phys. B **450**, 437 (1995) [arXiv:hep-th/9406003]; C. P. Korthals-Altes, S. Nicolis and J. Prades, Phys. Lett. B **316**, 339 (1993) [arXiv:hep-lat/9306017].

[17] A. Kehagias and K. Tamvakis, Phys. Lett. B **504** (2001) 38 [arXiv:hep-th/0010112].

[18] J. L. Cardy, Nucl. Phys. B **170**, 369 (1980); G. 't Hooft, Nucl. Phys. B **153**, 141 (1979; J. Groeneveld, J. Jurkiewicz and C. P. Korthals Altes, Phys. Lett. B **92**, 312 (1980).

[19] A. P. Gottlob and M. Hasenbusch, Physica A **201** (1993) 593.

[20] G. Arnold, B. Bunk, T. Lippert and K. Schilling, Nucl. Phys. Proc. Suppl. **119**, 864 (2003) [arXiv:hep-lat/0210010]; G. Arnold, T. Lippert, K. Schilling and T. Neuhaus, Nucl. Phys. Proc. Suppl. **94**, 651 (2001) [arXiv:hep-lat/0011058].